NASA Technical Memorandum 106087
ICOMP-93-08

Nonlinear Evolution of the First Mode Supersonic Oblique Waves in Compressible Boundary Layers. Part I – Heated/Cooled Walls

J.S.B. Gajjar
University of Manchester
Manchester, England

and Institute for Computational Mechanics in Propulsion
Lewis Research Center
Cleveland, Ohio

March 1993

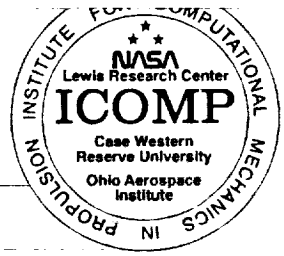

NASA

Nonlinear Evolution of the First Mode Supersonic Oblique Waves in Compressible Boundary Layers. Part-I Heated/Cooled Walls

J.S.B. Gajjar
Mathematics Department,
The University of Manchester,
Manchester, M13 9PL, England

Abstract

The nonlinear stability of an oblique mode propagating in a two-dimensional compressible boundary layer is considered under the long wave-length approximation. The growth rate of the wave is assumed to be small so that the ideas of unsteady nonlinear critical layers can be applied. It is shown that the spatial/temporal evolution of the mode is governed by a pair of coupled unsteady nonlinear equations for the disturbance vorticity and density. Expressions for the linear growth rate show clearly the effects of wall heating and cooling, and in particular how heating destabilises the boundary layer for these long wavelength inviscid modes at O(1) Mach numbers. A generalised expression for the linear growth rate is obtained and is shown to compare very well for a range of frequencies and wave-angles at moderate Mach numbers with full numerical solutions of the linear stability problem. The numerical solution of the nonlinear unsteady critical layer problem using a novel method based on Fourier decomposition and Chebychev collocation is discussed and some results are presented.

1. Introduction

One of the more important contributions to the linear stability of compressible boundary layers was the work of Lees & Lin (1946) who developed the inviscid theory and identified the different types of modes which exist in regions of relative subsonic and supersonic flow. This and subsequent modifications to the work to include viscous effects, is extensively described in the reviews by Reshotko (1976), and Mack (1984,1986) who also discusses the numerical results for the compressible linear stability problem. Recent work has concentrated on developing a more systematic approach, based on the the triple-deck type framework, and Smith(1989) discusses the lower- branch stability properties, whilst Gajjar & Cole (1989), Gajjar (1990), Cowley & Hall (1990), Brown & Smith (1990) consider the upper-branch and inviscid stability properties, with the last two papers concentrating more on the description of the acoustic and vorticity modes at high Mach numbers. The nonlinear stability properties, particularly of the inviscid modes, has however received scant attention, although exceptions include the paper by Goldstein & Wundrow (1990) which extends the Cowley & Hall work to include nonlinearity and also the work of Gajjar & Cole (1989,1992) who consider nonlinear neutral modes in compressible boundary layers, and Leib (1991) who has studied the evolution of modes in compressible shear layers.

One of the aims of this paper is to discuss the nonlinear evolution of the long wavelength inviscid modes in compressible boundary layers.

It is now well known that the critical layer where the phase speed of the disturbance wave is equal to the local flow velocity plays an important role in the stability of many shear and boundary layer flows. The ideas of nonlinear critical layers were first put forward by Benney & Begeron (1969) and Davies (1970) and they have been widely used in numerous papers since then. An excellent review of the many different aspects and properties of linear and nonlinear critical layers is given in the articles by Stewartson (1981) and Maslowe (1986). Benney & Bergeron showed how the properties of the nonlinear critical layer could be used to describe nonlinear neutral waves in parallel flows. This work has recently been extended to compressible boundary layer flows by Gajjar & Cole (1989), (hereafter referred to as I), Gajjar (1990), and Gajjar & Cole (1992), who obtain various results for the nonlinear neutral frequencies and wavenumbers which depend on the amplitude of the disturbance wave. All these results are based, however, on the underlying assumption that the neutral modes exist and that the critical layer is of an equilibrium type. Although a description of the nonlinear neutral structure is interesting, and provides a solution of the compressible Navier-Stokes equations, of more importance is the question of whether the assumed nonlinear neutral structure is stable and indeed attainable. This question and the relevance of the equilibrium critical layer to the overall stability picture has so far not been resolved and needs further consideration. In shear layers the far downstream asymptotic structure of the non-equilibrium critical layer bears close resemblance to Benney-Bergeron critical layer, although there are modifications stemming from unsteady effects and outer diffusion layers, Goldstein & Hultgren (1988).

Studies of the spatial evolution of waves on shear flows and in which the critical layer is of a non-equilibrium type have been conducted in a series of papers by Dr. Goldstein and his group, see for example Goldstein & Leib (1988), Goldstein & Hultgren (1988), Goldstein & Wundrow (1990). The nonlinearity studied in these papers is such that it induces a fully unsteady nonlinear critical layer problem whereas in other instances with weaker nonlinearity, the resulting evolution of the disturbance is described by an integro-differential equation of the Hickernell (1984) type, Goldstein & Leib (1990), Goldstein & Choi (1989), Leib (1991).

These papers demonstrate that even though spatial equilibration can occur in some instances, with the properties of a quasi-equilibrium critical layer coming into play, there are important differences between the equilibrium and non-equilibrium type approaches, see also Gajjar & Smith (1985). Comparisons of the theoretical predictions and experimental results for shear layers based on the latter approach show good agreement, Hultgren (1992). Mankbadi (1992ab) had also made extensive comparisons with experiments of the the incompressible weakly nonlinear theories for the Blasius boundary layer and his results

give convincing quantitative evidence that the unsteady nonlinear critical layer theories do indeed capture the early stages in the transition to turbulence of these flows.

Wu (1992) has studied the weakly nonlinear instability of Stokes layers using similar ideas and also obtained a novel generalisation of the Hickernell integro-differential equation by incorporating a weak spanwise dependence for the disturbance. Unsteady critical layer analysis has also been applied to study the evolution of waves in stratified flows, Churilov & Shukman (1988), and also in the flow over compliant surfaces, Gajjar (1991).

In this paper we consider the spatial/temporal evolution of an oblique mode propagating in a two-dimensional compressible boundary layer with non-insulated wall conditions. In Part II of this paper Gajjar (1992) the extension of this work to the insulated case for O(1) and also small Mach numbers is also described. In fact the generic problem there is essentially the same as that obtained here and can be retrieved also by taking a limit of the current problem. Long waves, based on the Rayleigh scalings, are considered and the growth rates are assumed to be small so that the ideas of nonlinear critical layers can be used. The mode is taken to grow slowly in the direction of propagation of the wave, and the cross variations are taken to be small and negligible. The assumptions made imply that the analysis here applies only to the evolution of the first mode, in the terminology of Mack (1984). The higher modes have much larger phase speeds and stem from regions of locally supersonic flow which require a modification to the present analysis.

In the following sections we analyse the disturbance quantities and obtain the governing nonlinear unsteady critical layer equations describing the evolution of the mode. It is shown below that the evolution is described by a pair of coupled equations for the disturbance vorticity and density, with the density acting as a source of the vorticity. These equations are essentially the unsteady counterparts of those obtained in I. The numerical solution of these equations using a novel method based on Fourier decomposition in the spanwise direction and Chebychev collocation in the normal direction is described also. The same notation and nondimensionalisation of I is used and in particular (x, y, z) denote the streamwise, normal and spanwise non-dimensional coordinates, (u, v, w) the corresponding velocities, t is the time, (p, ρ, T), are the nondimensional pressure, density and temperature respectively. The Reynolds number R is taken to be large throughout, M_∞ is the free-stream Mach number, and Γ is the ratio of specific heats. The basic flow is taken to be a flat plate or pressure gradient boundary layer with wall heating and cooling, see I also.

2. Problem Formulation

It is convenient to introduce Squire coordinates $(\xi, \bar{z})$ along and normal to the direction of propagation of the wave, with

$$\frac{\partial}{\partial x} \rightarrow R^{\frac{1}{2}}[\alpha(h\frac{\partial}{\partial \xi} + h^2\frac{\partial}{\partial X} - \beta h\frac{\partial}{\partial \bar{z}}],$$

$$\frac{\partial}{\partial z} \rightarrow R^{\frac{1}{3}}[\beta(h\frac{\partial}{\partial \xi} + h^2\frac{\partial}{\partial X}) + \alpha h\frac{\partial}{\partial \bar{z}}],$$

$$\frac{\partial}{\partial t} \rightarrow h^2 R^{\frac{1}{3}}(-\alpha c - h\sigma)\frac{\partial}{\partial \xi},$$

and $\xi = R^{\frac{1}{3}}h(\alpha x + \beta z - \alpha c h t), \bar{z} = R^{\frac{1}{3}}h(\alpha z - \beta x)$, and $X = R^{\frac{1}{3}}h^2(\alpha x + \beta z)$, with the wave growing on the slow X scale. The scale factor $h, (h << 1)$ is introduced so that we are considering long waves on the Rayleigh scalings. The growth rates are thus of $O(h^2)$. Also c is the phase speed of the wave, σ is taken to be real and $\alpha = \cos\theta, \beta = \sin\theta$, where θ is the direction of propagation of the wave. With respect to the Squire coordinates we have the corresponding velocities $\bar{u} = \alpha u + \beta w, \bar{w} = -\beta u + \alpha w$. The basic flow is taken to a two-dimensional boundary layer flow with

$$(u, v, w) = (U_B(x, Y), O(R^{-\frac{1}{3}}), 0), p = p_B = 1/\Gamma M_\infty^2,$$

$$T = T_B(x, Y), \rho = \rho_B(x, Y) = 1/T_B,$$

where $y = R^{-\frac{1}{3}}Y$ and we assume also that

$$U_B, \rho_B, \rightarrow 1 \quad \text{as} \quad Y \rightarrow \infty,$$

$$U_B \sim \lambda_1 Y + \lambda_2 Y^2 + \ldots \quad \text{as} \quad Y \rightarrow 0+,$$
$$\rho_B \sim R_0 + R_1 Y + \ldots \quad \text{as} \quad Y \rightarrow 0+,$$
$$T_B \sim S_0 + S_1 Y + \ldots \quad \text{as} \quad Y \rightarrow 0+.$$

Small disturbances of size δ are introduced and expansions for the disturbance quantities are considered in each of the regions, see Fig. 1. The disturbance size $\delta = O(h^3)$ has been anticipated below to allow the nonlinearity and unsteadiness to appear in the critical layer.

Firstly in the region $Y = O(1)$ the various flow quantities expand as

$$\begin{aligned}
\bar{u} &= \alpha U_B + h^3\tilde{u}_1 + h^4\tilde{u}_2 + \ldots, \\
v &= h^4\tilde{v}_1 + h^5\tilde{v}_2, \\
\bar{w} &= -\beta U_B + h^3\tilde{w}_1 + h^4\tilde{w}_2 + \ldots, \\
p &= p_B + h^4\tilde{p}_1 + h^5\tilde{p}_2 + \ldots, \\
\rho &= \rho_B + h^3\tilde{\rho}_1 + h^4\tilde{\rho}_2 + \ldots,
\end{aligned} \tag{2.1}$$

and these are taken to be independent of $\bar{z}$ to this order. Substitution of (2.1) into the Navier- Stokes equations yields at leading order the solutions,

$$\tilde{u}_1 = \tilde{A}_0 \alpha U_{BY}, \quad \tilde{v}_1 = -\alpha \tilde{A}_{0\xi} U_B, \quad \tilde{p}_1 = \tilde{P}_1,$$

$$\tilde{\rho}_1 = \tilde{A}_0 \rho_{BY}, \quad \tilde{w} = -\beta \tilde{A}_0 U_{BY}, \tag{2.2}$$

where $\tilde{A}_0 = \tilde{A}(X)e^{i\gamma\xi} + c.c.$, $\tilde{P}_1 = \tilde{P}(X)e^{i\gamma\xi} + c.c.$and $\tilde{A}$, $\tilde{P}$ are slowly varying amplitude functions, and γ is the wavenumber of the oblique mode. At the next order the solutions

$$\tilde{v}_2 = \frac{U_B}{\alpha} \int^Y \frac{\tilde{p}_{1\xi}}{\rho_B U_B^2}\, dy + c\alpha \tilde{A}_{0\xi} + \tilde{A}_1 U_B - \frac{\tilde{p}_{1\xi} \alpha Y U_B}{\Gamma p_B},$$

$$\tilde{p}_2 = \tilde{P}_2 - \int_0^Y \alpha U_B \rho_B \tilde{v}_{1\xi}\, dy, \tag{2.3}$$

and

$$\tilde{u}_{2\xi} = -\tilde{u}_{1X} - \tilde{v}_{2Y} - \frac{\alpha U_B \tilde{p}_{1\xi}}{\Gamma p_B},$$

are obtained and $\tilde{A}_1$, $\tilde{P}_1$ are unknown function of ξ and X.

In region Z2 where $Y = h\bar{Y}$, the properties of the basic flow in (2.1) and the solutions (2.2),(2.3) imply the expansions

$$\bar{u} = \alpha(h\lambda_1 \bar{Y} + h^2 \lambda_2 \bar{Y}^2) + h^3 u_1 + h^4 u_2 + \ldots,$$

$$v = h^5 v_1 + h^6 v_2 + \ldots,$$

$$\bar{w} = -\beta(h\lambda_1 \bar{Y} + h^2 \lambda_2 \bar{Y}^2) + h^3 w_1 + h^4 w_2 + \ldots,$$

$$p = p_B + h^4 p_1 + h^5 p_2 + \ldots,$$

$$\rho = R_0 + hR_1 \bar{Y} + h^2 R_2 \bar{Y}^2 + h^3 \rho_1 + h^4 \rho_2 + \ldots.$$

Substituting into the equations and solving gives

$$v_1 = -\alpha \tilde{A}_{0\xi} \lambda_1 \bar{Y}, \quad u_1 = \alpha \lambda_1 \tilde{A}_0, \quad w_1 = -\frac{\beta \lambda_1^2 \bar{Y} \tilde{A}_0}{(\lambda_1 \bar{Y} - c)}, \quad \rho_1 = \frac{R_1 \lambda_1 \bar{Y} \tilde{A}_0}{(\lambda_1 \bar{Y} - c)}$$

$$\begin{aligned} v_2 = {} & \frac{\sigma u_{1\xi} - \alpha c u_{1X}}{\alpha \lambda_1} - \frac{\alpha \lambda_1 \lambda_2 \tilde{A}_{0\xi}}{\lambda_1^3}[\bar{\eta}^2 - c^2] + \frac{p_{1\xi} R_1 c}{\alpha R_0^2 \lambda_1^2} \\ & - \frac{(p_{2\xi} + p_{1X})}{R_0 \alpha_0 \lambda_1} - \frac{\alpha c \tilde{A}_{0\xi}}{\lambda_1}[\frac{2\lambda_2}{\lambda_1} + \frac{R_1}{R_0}]\bar{\eta}[\ln|\bar{\eta}| + \phi^{\pm}], \end{aligned} \tag{2.4}$$

where $\bar{\eta} = (\lambda_1 \bar{Y} - c)$. In the above we have anticipated the condition that the normal velocity is zero at the wall which leads to relation (from the solution for v_1) that

$$p_1 = R_0 \lambda_1 \alpha^2 c \tilde{A}_0.$$

These solutions show that the density, temperature and spanwise fluctuations become algebraically singular in the critical layer. The $\phi^{\pm}$ terms are jump conditions arising from the continuation across the critical layer at $\bar{\eta} = 0$. Before discussing the critical layer equations it is convenient to consider first the outer potential flow region Z3 and derive the amplitude equation describing the evolution of the mode.

In region Z3 with $Y = \hat{Y}/h$ we have the expansions

$$\bar{u} = \alpha + h^4\bar{u}_1 + h^5\bar{u}_2 + \ldots,$$

$$v = h^4\bar{v}_1 + h^5\bar{v}_2 + \ldots,$$

$$\bar{w} = -\beta + h^4\bar{w}_1 + h^5\bar{w}_2 + \ldots,$$

$$\rho = 1 + h^4\bar{\rho}_1 + \ldots,$$

$$p = p_B + h^4\bar{p}_1 + h^5\bar{p}_2 + \ldots.$$

When substituted into the Navier-Stokes equations the equation for $\bar{p}_1$ is just the Prandtl-Glauert equation which yields

$$\bar{p}_1 = P_{10}e^{-\gamma\Omega\hat{Y}}e^{i\gamma\xi}, \quad \bar{v}_1 = \frac{\bar{p}_1\Omega}{i\alpha}, \tag{2.5}$$

where real quantities are assumed, P_{10} is an unknown function of X and

$$\Omega \equiv (1 - \frac{\alpha^2}{\Gamma p_B})^{\frac{1}{2}} = (1 - \cos^2\theta M_\infty^2)^{\frac{1}{2}}.$$

At the next order the $e^{i\gamma\xi}$ component of $\bar{p}_2$, say P_{21} is given by

$$P_{21} = -\frac{c\gamma(1-\Omega^2)}{2\Omega}P_{10}\hat{Y}e^{-\gamma\Omega\hat{Y}} + \hat{Y}P_{10X}i\Omega e^{-\gamma\Omega\hat{Y}} + \bar{P}_{21}e^{-\gamma\Omega\hat{Y}},$$

and the $e^{i\gamma\xi}$ componenet of $\bar{v}_2$, V_{21} satisfies

$$i\alpha\gamma V_{21}|_{\hat{Y}=0} = \frac{c\gamma(1+\Omega^2)}{2\Omega}P_{10} + \gamma\Omega\bar{P}_{21}. \tag{2.6}$$

3. Derivation of the amplitude equation

The amplitude equation is derived by matching between the different regions and also imposing the condition that the normal velocity is zero. At leading order from (2.4) and (2.5) we get

$$P_{10} = \alpha^2\lambda_1\tilde{A}R_0c = \frac{\gamma\alpha^2\tilde{A}}{\Omega}. \tag{3.1}$$

which gives the dispersion relation

$$\gamma = \Omega\lambda_1 R_0 c = \lambda_1 R_0 c(1-\cos^2\theta M_\infty^2)^{\frac{1}{2}}. \tag{3.2}$$

Denoting the $e^{i\gamma\xi}$ components of $\tilde{p}_2, \tilde{A}_1, \tilde{A}_0\phi^{\pm}$ by $\tilde{P}_{21}, \tilde{A}_{11}$ and $\tilde{A}\phi_1^{\pm}$ respectively matching of the normal velocities and pressure between Z1 and Z3 gives using (2.3) the relations

$$V_{21}|_{\hat{Y}=0} = \frac{i\gamma}{\alpha}P_{10}I_1 + i\gamma\alpha c\tilde{A} + \tilde{A}_{11},$$

$$\tilde{P}_{21} = \tilde{P}_{21} - \alpha^2\gamma^2\tilde{A}I_2, \tag{3.3}$$

where

$$I_1 = \int_0^\infty [\frac{1}{\rho_B U_B^2} - \frac{1}{R_0\lambda_1^2 y^2} + \frac{1}{R_0\lambda_1^2 y}(\frac{R_1}{R_0} + \frac{2\lambda_2}{\lambda_1}) - 1]\, dy,$$

and

$$I_2 = \int_0^\infty (\rho_B U_B^2 - 1)\, dy.$$

Matching the normal velocities in Z1 and Z2 gives from (2.3-2.4),

$$-\frac{i\gamma P_{10}\lambda_2}{\alpha R_0\lambda_1^2} + \tilde{A}_{11}\lambda_1 = -\frac{i\alpha c\gamma\tilde{A}}{\lambda_1}(\frac{2\lambda_2}{\lambda_1} + \frac{R_1}{R_0})\lambda_1\phi_1^+ + \frac{2i\lambda_2\alpha\gamma c\tilde{A}}{\lambda_1}. \tag{3.4}$$

Next setting the second order component of the normal velocity in Z2 to zero at the wall gives from (2.4),

$$iD_1\tilde{A} - \alpha c\tilde{A}_X - \frac{1}{R_0\alpha_0\lambda_1}P_{10X} - \frac{i\gamma}{R_0\alpha\lambda_1}\tilde{P}_{21} + \frac{i\gamma\alpha c^2}{\lambda_1}(\frac{2\lambda_2}{\lambda_1} + \frac{R_1}{R_0})\phi_1^-\tilde{A} = 0. \tag{3.5}$$

where

$$D_1 = \gamma\sigma + \frac{\gamma R_1 c}{\alpha R_0^2\lambda_1^2}(\frac{P_{10}}{\tilde{A}}) + \frac{\gamma c^2\alpha}{\lambda_1}(\frac{2\lambda_2}{\lambda_1} + \frac{R_1}{R_0})\ln|c|.$$

Finally eliminating $\tilde{P}_{21}, \tilde{A}_{11}$ using (2.6), (3.1-3.5) leads to the amplitude equation

$$iD_4\tilde{A} - 2c\alpha\tilde{A}_X - \frac{i\gamma\tilde{A}\alpha c^2}{\lambda_1}(\frac{2\lambda_2}{\lambda_1} + \frac{R_1}{R_0})(\phi_1^+ - \phi_1^-) = 0, \tag{3.6}$$

where the D_i are given by

$$D_2 = \frac{c\gamma(1+\Omega^2)}{2\Omega}(\frac{P_{10}}{\tilde{A}}) - \gamma^3\Omega\alpha^2 I_2 + \gamma^2\alpha^2 c + \gamma^2 I_1(\frac{P_{10}}{\tilde{A}}),$$

$$D_3 = \frac{1}{\gamma\Omega}[-D_2 - \frac{2\alpha^2\gamma^2\lambda_2 c}{\lambda_1^2} - \frac{\gamma^2\lambda_2}{\lambda_1^3 R_0}(\frac{P_{10}}{\tilde{A}})],$$

and

$$D_4 = D_1 - \frac{\gamma}{R_0\alpha_0\lambda_1}D_3.$$

Note that D_4 is a real quantity.

The jump conditions $(\phi_1^+ - \phi_1^-)$ are determined from the properties of the critical layer and this is considered next.

4. The critical layer equations

Expansions for the critical layer follow readily from the solutions and expansions in Z2. In the critical layer with $Y = \frac{hc}{\lambda_1} + h^2\eta$, we have

$$\bar{u} = \alpha[hc + h^2(\lambda_1\eta + \frac{\lambda_2 c^2}{\lambda_1^2})] + h^3U_1 + h^4U_2 + \ldots,$$

$$v = h^5V_0 + h^6V_1 + h^7V_2 + \ldots,$$

$$\bar{w} = -\beta hc + h^2W_1 + \ldots,$$

$$p = p_B + h^4P_1 + h^5P_2 + \ldots,$$

$$\rho = R_0 + h\frac{R_1 c}{\lambda_1} + h^2\pi_1 + \ldots.$$

Substitution into the equations shows that the pressure is the same as outside the critical layer. The leading order solution for the normal velocity yields

$$R_0\alpha\lambda_1 V_0 = -P_{1\xi}.$$

The first nontrivial solutions lead to the critical layer equations

$$L\pi_1 = 0, \quad L\tilde{Q}_2 = \frac{\pi_{1\eta}P_{1\xi}}{R_0^2}, \tag{4.1}$$

where the $\tilde{Q} = U_{2\eta}$ and the operator L is defined by

$$L \equiv \alpha(\lambda_1\eta + \frac{\lambda_2 c^2}{\lambda_1^2} - \frac{\sigma}{\alpha})\frac{\partial}{\partial\xi} + \alpha c\frac{\partial}{\partial X} + V_0\frac{\partial}{\partial\eta}.$$

In order to match with the solutions outside we need

$$\pi_1 \sim R_1\eta + \frac{2R_1 c}{\lambda_1\eta}Re(\tilde{A}e^{i\gamma\xi}) + \ldots,$$

$$\tilde{Q}_2 \sim 2\alpha\lambda_2\eta + \frac{2\alpha c}{\eta}(\frac{2\lambda_2}{\lambda_1} + \frac{R_1}{R_0})Re(\tilde{A}e^{i\gamma\xi}) + \ldots, \tag{4.2}$$

as $\eta \to \pm\infty$. Here Re denotes the real part. Hence the evolution of the mode is governed by the solution of the equations (4.1) together with the amplitude equation (3.6). Using (4.2) the amplitude equation can be written in the form

$$iD_4\tilde{A} - 2\alpha c\tilde{A}_X - \frac{i\gamma^2 c}{2\pi\lambda_1}\int_0^{\frac{2\pi}{\gamma}}\int_\infty^\infty \tilde{Q}_2 e^{-i\gamma\xi}\,d\eta\,d\xi = 0. \tag{4.3}$$

The D_4 term in (3.9) and (4.3) gives a correction to the wavenumber and can be in effect be removed by redefining ξ, and is thus set to zero. Note that this also fixes σ and hence the correction to the frequency.

A more standard form of the equations can be obtained by renormalising with the scalings

$$\lambda_1\eta + \frac{\lambda_2 c^2}{\lambda_1^2} - \frac{\sigma}{\alpha} = \lambda_1 d_1^* Z,$$

$$\pi_1 = R_1 d_1^* \Pi, \quad X = \frac{c}{\lambda_1\gamma d_1^*}\bar{X} - \bar{X}_0,$$

$$\gamma\xi = \xi^* + \xi_0, \quad \tilde{A} = d_0^* A e^{-i\xi_0}, \quad \tilde{Q}_2 = d_2^* Q,$$

where

$$d_0^* = \frac{c^3}{8\lambda_1^3}\left(\frac{2\lambda_2}{\lambda_1} + \frac{R_1}{R_0}\right)^3, d_1^* = \left(\frac{2cd_0^*}{\lambda_1}\right)^{\frac{1}{3}},$$

$$d_2^* = \frac{2\alpha c d_0^*}{d_1^*}\left(\frac{2\lambda_2}{\lambda_1} + \frac{R_1}{R_0}\right),$$

$$J = \frac{\frac{R_1}{R_0}}{\left(\frac{2\lambda_2}{\lambda_1} + \frac{R_1}{R_0}\right)},$$

to give

$$\frac{\partial Q}{\partial\bar{X}} + Z\frac{\partial Q}{\partial\xi^*} - Re(iAe^{i\xi^*})\frac{\partial Q}{\partial Z} = JRe(iAe^{i\xi^*})\frac{\partial\Pi}{\partial Z},$$

$$\frac{\partial\Pi}{\partial\bar{X}} + Z\frac{\partial\Pi}{\partial\xi^*} - Re(iAe^{i\xi^*})\frac{\partial\Pi}{\partial Z} = 0. \tag{4.4ab}$$

Also the boundary conditions (4.2) and the amplitude equation (4.3) reduce to

$$Q \sim (1-J)Z + \frac{Re(Ae^{i\xi^*})}{Z} + \ldots \text{ as } Z \to \pm\infty,$$

$$\Pi \sim Z + \frac{Re(Ae^{i\xi^*})}{Z} + \ldots \text{ as } Z \to \pm\infty, \tag{4.5}$$

and

$$A_{\bar{X}} = -\frac{i}{\pi}\int_0^{2\pi}\int_{-\infty}^{\infty} Qe^{-i\xi^*}\, d\xi^*\, dZ. \tag{4.6}$$

The constants $\bar{X}_0, \xi_0$ can be chosen to match upstream conditions and $A \rightarrow e^{\pi\bar{X}}$ far upstream ($\bar{X} \rightarrow -\infty$), where the scaled linear growth rate is now π.

The problem (4.3-4.6) is similar to that obtained by Goldstein & Wundrow (1990) in their investigation of the stability of hypersonic boundary layers. Note that viscous effects have been neglected above which means that the scale factor h is such that $h >> O(R^{-\frac{1}{14}})$. If $h = O(R^{-\frac{1}{14}})$ (4.4) is modified to

$$\bar{L}(Q) = JRe(iAe^{i\xi^*})\frac{\partial \Pi}{\partial Z} + \gamma_c\frac{\partial^2 Q}{\partial Z^2} + \gamma_e\frac{\partial^2 \Pi}{\partial Z^2},$$

$$\bar{L}(\Pi) = \gamma_d\frac{\partial^2 \Pi}{\partial Z^2}, \tag{4.7ab}$$

where the operator $\bar{L}$ is defined by

$$\bar{L} \equiv \frac{\partial}{\partial \bar{X}} + Z\frac{\partial}{\partial \xi^*} - Re(iAe^{i\xi^*})\frac{\partial}{\partial Z},$$

and the parameters $\gamma_c, \gamma_d, \gamma_e$ are dependent on the viscosity law used. With the inclusion of viscosity the wavenumbers are in effect $O(R^{\frac{3}{7}})$. We also have

$$\gamma_c = \frac{S_0\mu(S_0)R^{-\frac{1}{2}}h^{-7}}{\gamma\alpha\lambda_1 d_1^{*3}}, \quad \gamma_d = \gamma_c/Pr,$$
$$\gamma_e = \gamma_d J(\frac{Pr\mu'(S_0)}{R_0\mu(S_0)} - 1), \tag{4.8}$$

where Pr is the (constant) Prandtl number and $\mu(T)$ is the viscosity law. The properties of the steady state or equilibrium version of (4.7) with $\gamma_e = 0$ are discussed by Gajjar & Cole (1989).

It can be seen from the above scalings and (4.8) that as far as the oblique-wave is concerned, the θ dependence can be scaled out of the inviscid problem, but not for the viscous problem. In fact the more oblique the wave the larger the effective viscosity for fixed values of the other parameters.

For an insulated flat plate boundary layer the same normalized problem (4.4) is obtained, although the J parameter is the limit of that given here as R_1 tends to zero, see Gajjar (1992). We note also that Wundrow (1989) has obtained equations similar to (4.7) in his study of the stability of compressible mixing layers and he presents several numerical results.

Linear growth rate.

For the linear problem the standard jump conditions of $i\pi$ across the critical layer when substituted into (3.6) determines the linear growth rate as

$$\kappa_r = \frac{\gamma c \pi}{2\lambda_1}\left(\frac{2\lambda_2}{\lambda_1} + \frac{R_1}{R_0}\right). \tag{4.9}$$

A more useful form for the growth rate, wavenumber and frequency can be obtained by first recasting the various expression in unscaled form i.e. without the h factors present. From the multiple scaling used it can be seen that the effective wavenumber, frequency, and growth rate are given by

wavenumber: $R^{\frac{1}{2}}\gamma_* = R^{\frac{1}{2}}(\gamma h + \ldots)$, frequency: $R^{\frac{1}{2}}\omega_* = R^{\frac{1}{2}}(\gamma h^2 c\cos\theta + \ldots)$,

growth rate: $R^{\frac{1}{2}}\kappa_* = R^{\frac{1}{2}}(\kappa_r h^2 + \ldots)$, phase-speed: $c_* = \dfrac{\omega_*}{\gamma_*\cos\theta}$.

For the flat plate boundary layer flow, taking the Prandtl number to be unity, the basic flow is given by in Dorodnitsyn-Howarth variables,

$$U_B(x,Y) = f'(\eta), \quad (2x)^{\frac{1}{2}}\eta = \int_0^Y \rho_B\, dY$$

where $f(\eta)$ satisfies the equation

$$(\mu(T_B)\rho_B f'')' + ff'' = 0, \quad f(0) = f'(0) = 0, f'(\infty) = 1,$$

and

$$\frac{1}{\rho_B} = T_B = (1-t_b)U_B + t_b + \frac{1}{2}(\Gamma-1)M_\infty^2(t_b + U_B)(1-U_B).$$

Here t_b is related to the wall temperature T_W by

$$T_W = (1 + \frac{1}{2}M_\infty^2(\Gamma-1))t_b$$

and $\mu(T_B)$ is the viscosity law. In particular $t_b = 1$ corresponds to the case for insulated walls.

The above asymptotic expressions for the wavenumber (3.2) and growth rate (4.9) thus reduce to

$$\gamma_*^2 = \frac{\omega_* R_0^2 f''(0)}{\sqrt{2}\cos\theta}(1 - M_\infty^2\cos^2\theta)^{\frac{1}{2}}, \tag{4.10}$$

$$\kappa_* = -\frac{\omega_*\pi}{\cos\theta}\left(\frac{1-t_b}{t_b}\right)\left(1 + \frac{\frac{d(\mu(T_B)\rho_B)}{dT_B}T_W}{2\mu(T_B)\rho_B}\right)_{\eta=0}. \tag{4.11a}$$

The expressions (4.10), (4.11a) give the leading terms in the asymptotic expansion for the wavenumber and growth rate in terms of the frequency in this long wavelength approximation. It is seen that for heated walls, with $t_b > 1$ the growth rate is positive and the

growth rate increases with increasing wall heating. Also the above expression shows that for fixed frequencies the oblique waves have larger growth rates than the 2D modes.

Clearly when $t_b = 1$ i.e for the insulated case, the growth rate reduces to $O(h^3)$. The insulated case is considered in Part II of this paper Gajjar (1992), where it is shown that for O(1) Mach numbers, the growth rate term is given by

$$\kappa_* = \frac{\pi\omega_*^2(\Gamma-1)M_\infty^2}{T_W\cos^2\theta\gamma_*}\left(1+\frac{\frac{d(\mu(T_B)\rho_B)}{dT_B}T_W}{2\mu(T_B)\rho_B}\right)_{\eta=0}. \tag{4.11b}$$

Further when the Mach number is much smaller of $O(h^{\frac{1}{2}})$ then the growth rate reduces to $O(h^4)$ and the λ_4 contribution comes into play. In this case κ_* above is modified to

$$\kappa_* = \frac{\pi\omega_*^2}{\cos^2\theta\gamma_*}\left[\frac{(\Gamma-1)M_\infty^2}{T_W}\left(1+\frac{\frac{d(\mu(T_B)\rho_B)}{dT_B}T_W}{2\mu(T_B)\rho_B}\right)-\frac{c*}{4(\mu(T_B)\rho_B)f''(0)^2}\right]_{\eta=0}. \tag{4.11c}$$

The above expressions taken together show that for long waves, for insulated or isothermal walls, a generalised expression for the growth rate asymptotically valid to much higher order is

$$\kappa_* = \frac{\omega_*\pi}{2DU_B^2\rho_B\cos\theta}D(\rho_B DU_B) \tag{4.12a}$$

where $D = d/dY$ and ρ_B, DU_B, $D(\rho_B DU_B)$ are evaluated at $Y = Y_c$. The expression (4.12a) reduces to (4.11) by expanding the various quantities in (4.12a) and noting that for small c_*, $Y_c = c_*/\lambda_1$ to a good approximation. For neutral modes (4.11c) agrees with that given in I.

From (3.2) a leading order expression for the frequency is given by

$$\omega_* = c_*^2\cos\theta DU_B\rho_B(1-\cos^2\theta M_\infty^2)^{\frac{1}{2}}. \tag{4.12b}$$

The growth rates as computed from (4.11), (4.12a) are compared with numerically computed values from the solution of the linear compressible Rayleigh problem* and the results are shown in Figures 2-4. The Sutherland viscosity law $\mu(T) = \dfrac{T^{3/2}}{(0.5+T)}$ together with $\Gamma = 1.4$ was used in these comparisons. The growth rates are plotted against the phase-speed because, for fixed frequencies the phase-speed as computed from (4.12b) would not be particularly accurate as (4.12b) is derived from just the leading order expression for the wavenumber. Using the phase-speed as a parameter and computing the other quantities from the various expressions written in terms of c_* gives a much more meaningful comparison. It is seen, Fig. 2(a-d), that for the non-insulated case whereas the formal

* The author would like to thank Dr. L. Hultgren for providing the code used in the computation of the inviscid spatial eigenvalues.

leading order asymptote (4.11a) works well only for low Mach numbers and very low frequencies, the generalised expression give excellent agreement for a range of frequencies and oblique angles upto moderately supersonic Mach numbers. Figures 3(a-e) show the comparisons for the insulated case also. The expression (4.11c) and the generalised form (4.12a) again give excellent agreement with the full solutions for the same range of Mach numbers. For increasing Mach numbers the critical layer moves away from the wall and the assumptions used in deriving (4.11), (4.12a) become less valid. Comparisons of the asymptotic expression for the wavenumber against numerically computed values in Figures 4(a-f) show that the leading order asymptote works well only for small c_* and further terms would need to be incorporated for a better comparison.

5. Numerical solution.

The method used to solve (4.5-4.7) is different from that used previously and is described below. The method was developed so that the calculations could be carried on the AMT DAP-510 machine which is a massively parallel SIMD system comprising 1024 processors arranged in a 32 by 32 matrix. Since the individual processors of this machine are relatively slow, the machine is most efficient only when the underlying algorithm is highly parallel a feature of the current method.

The vorticity Q and density Π were decomposed into individual Fourier modes by writing

$$Q = (1-J)Z + (\frac{1}{2}\sum_{0}^{\infty} Q_n e^{in\xi^*} + c.c),$$

$$\Pi = Z + (\frac{1}{2}\sum_{0}^{\infty} \Pi_n e^{in\xi^*} + c.c)$$

to give a set of equations for the Q_n, Π_n similar to those given in Goldstein & Hultgren (1988). The system was truncated to solve for $(N+1)$ Fourier modes and a predictor corrector scheme was used to advance in time. The resulting equations at a particular time level $(j+1)$ are then of the form

$$Q_k^{j+1} + ikZQ_k^{j+1} - \gamma_c Q_{kZZ}^{j+1} = r_k, \tag{5.1}$$

for each Fourier mode Q_k, $(k = 0, ..., N)$ and the nonlinear contributions are contained in the r_k term on the right hand side. These were then solved using Chebychev collocation, by first mapping the infinite interval into [-1,1] with the transformation

$$Z = 2y/\sqrt{1-y^2},$$

and writing

$$Q_k^{j+1} = \sum_{l=0}^{M} a_l^{(k)} T_l(y),$$

to give from (5.1) a set of linear equations for the Chebychev coefficeints $a_l^{(k)}$. The inverses of the coefficent matrices were pre-computed and stored, and the $a_l^{(k)}$ were obtained by doing matrix-vector multiplications for each Fourier mode. The method is thus fully vectorizable/parallelizable and suitable for massively parallel systems like the AMT DAP-510.

Note that since the infinite region is mapped into the finite region [-1,1] the Haynes (1985) procedure does not need to be used. Another advantage of the method is that full spectral accuracy in ξ^* and Z is obtained. As described above the method requires the pre-computation and storage of $(N+1)$ complex $(M+1)$ by $(M+1)$ matrices, since as (5.1) shows the differential operator involves an explicit dependence on k with the ikZ term. A modification of the method was used to avoid the large storage problems by writing (5.1) in the form

$$Q_k^{j+1} + iNZQ_k^{j+1} - \gamma_c Q_{kZZ}^{j+1} = i(N-k)ZQ_k + r_k.$$

This worked quite well in practice.

One final point is the evaluation of the integral in the scaled amplitude equation

$$A_{\tilde{X}} = -i \int_{-\infty}^{\infty} Q_1 \, dZ. \tag{5.2}$$

With the mapping the integral becomes

$$\int_{-1}^{1} Q_1 \frac{dZ}{dy} \, dy,$$

and was evaluated using Gaussian quadrature with the Chebychev poylnomials as basis functions. The quadrature points $q_j = \cos(\frac{(2j-1)\pi}{2n})$, $j = 1,...,n$ were used in the evaluation of the integral as this avoids difficulties at the endpoints $y = \pm 1$. This too can be implemented quite efficiently as a matrix vector multiplication.

6. Results and discussion

The numerical method was first tested by computing some test cases of the Goldstein & Hultgren (1988) problem for shear layers. (This corresponds to taking $\Pi = 0, J = 0$ in (4.7) together with an additional term $\frac{U}{2}\frac{dA}{d\tilde{X}}$ on the right hand side of (4.7a), see equation (3.16) of Goldstein & Hultgren (1988)). Some sample results are shown in Figures 5(a-d) and these are in excellent agreement with those of Goldstein & Hultgren (1988) and Goldstein & Leib (1988). It was found necessary to use a large number of Chebychev modes in the normal direction, typically 150 modes, together with very small timesteps, especially for the inviscid cases, in order to reproduce the results. One reason for this is that as the

disturbance evolves downstream, the vorticity develops into the familiar cat's eyes pattern and therefore many modes are required to resolve the very thin shear layers which form. The calculations were quite sensitive to the accurate computation of the integral in (5.2) and here 120 modes were needed for the later stages of the evolution of the disturbance.

Some results for the current problem (4.7) are shown in Figures 6-7. To reduce the number of parameters in (4.7) the Prandtl number was taken to be unity and the Chapman viscosity law was used giving $\gamma_e = 0$. For J zero or small and positive, Figures 6(a-d), the results are similar to those of the shear layer calculations, Figure 5, see also Goldstein & Hultgren (1988). The growth rate of the wave follows the linear value closely and then decreases as the nonlinear terms become more dominant. The $J = 0$ case is also a special case of that arising in the instability of the flow over compliant surfaces, Gajjar(1991). In Figure 6d we show the effect of inputting incorrect initial conditions. The growth rate after rapid oscillations settles down to its correct linear value. For larger values of J positive, Figure 7 the growth rate decreases initially from the linear value but far downstream this is reversed and very large fluctuations are present. The effect of viscosity can be seen in Figures 7 which show that the smaller the viscosity parameter γ_c the greater the effect on the amplitude in the nonlinear regime. In figure with $\gamma_c = 1$ the disturbance reaches a large amplitude and then settles down with small oscillations about this amplitude. For a smaller value of $\gamma_c = 0.5$, in Figure 7(c,d) it is seen that after reaching a peak amplitude the effect of nonlinearity and the forcing from the density causes very large fluctuations in the amplitude. Near $\bar{X} = 3$ the amplitude drops rapidly and then increases again with the decrease/increase taking place within a short X-scale.

The computations in Figures 6,7 do not go far enough in $\bar{X}$ to be able to ascertain what the the limiting properties of the downstream evolution are, although judging from the work of Goldstein & Hultgren (1989), it is expected that the properties of equilibrium compressible critical layers as dicusssed in Gajjar & Cole (1989) do come into play at some stage with outer diffusion layers also present. This however requires further analysis and more extensive numerical computations of the nonlinear problem. The nonlinear calculations require considerable resources, especially the computations with small viscosity where very small timesteps are necessary to allow a stable calculation.

Acknowledgement

The author gratefully acknowledges the support of ICOMP, NASA Lewis Research Center, Cleveland, where part of this work was done (in 1990, 1991), and would like to thank the Science and Engineering Research Council of G.B. for the AMT DAP-510 facility purchased under grant no. GR/E7072.6 . Dr's M. Goldstein, Hultgren, Leib and Wundrow are thanked for their helpful comments.

References

Benney, D. J., and Bergeron, R. F. *Studies in Appl. Math.*, **48** (1969), 181.

Churilov, S.M. & Shukman, I.G., *Jour. Fluid Mech.*,, (1988), 187.

Cowley, S. J. and Hall, P., *Jour. Fluid Mech.*, **214** (1990), 17.

Davies, R.E., *Jour. Fluid Mech.*, **36** (1969), 337.

Gajjar, J. S. B., and Cole, J. W., *Theo. Comp. Fluid Dyn.*, **1** (1989), 105.

Gajjar, J. S. B., in *'Proc of the ICASE/Langley workshop on Stability and Transition'* (eds. M.Y. Hussaini and R.G. Voigt) (1990).

Gajjar, J. S.B., in *'Recent Developments in Turbulence Management'*, ed. K.S. Choi, (1991) Kluwer Pub.

Gajjar, J. S. B., and Cole, J. W., *in preparation*, (1992).

Gajjar, J. S. B., *in preparation*, (1992)

Gajjar, J. S. B., and Smith, F. T., *Jour. Fluid Mech.*, **157** (1985), 53.

Goldstein, M. E., and Choi, K. S., *Jour. Fluid Mech.*, (1989), **207**, 97, (see also *Corrigendum Jour. Fluid Mech.*, **216**, 659.

Goldstein, M. E., and Hultgren, L. S., *Jour. Fluid Mech.*, **197** (1988), 295.

Goldstein, M. E., and Leib, S. J., *Jour. Fluid Mech.* **191** (1988), 481.

Goldstein, M. E., and Wundrow, D. W., *Jour. Fluid Mech.*, **219** (1990), 585.

Haynes, P., *Jour. Fluid Mech.*, **161** (1985), 493.

Hickernell, F. J. *Jour. Fluid Mech.*, **142** (1984), 431.

Hultgren, L. S., *Jour. Fluid Mech.*, (1992) **236**, 635.

Leib, S. J., *Jour. Fluid Mech.*, (1991), **224**, 551.

Lees, L., and Lin, C. C., NASA Tech. Note No. 1115 (1946)

Mack, L. M., AGARD Rep. no 709, (1984).

Mack, L. M., in *'Stability of Time Dependent and Spatially Varying Flows'* (ed. D. L. Dwoyer and M. Y. Hussaini), Springer, (1987)

Mankbadi, R. M., *submitted to the Jour. Fluid Mech.*, (1992ab)

Maslowe, S., Ann. Rev. Fluid Mech., **18** (1986), 405.

Reshotko, E., *Ann Rev Fluid Mech.* **8** (1976), 311.

Smith, F. T. *Jour. Fluid Mech.*, **198** (1989), 127.

Smith, F. T., and Brown, S. N., *Jour. Fluid Mech.*, **219** (1990), 499.

Stewartson, K., *I.M.A. Jour. Appl. Math.*, **27** (1981), 133.

Wu, X., Ph.D. Thesis Univ. of London, (1992).

Wundrow, D. M., Ph. D. Thesis, State Univ. of New York at Buffalo, (1989).

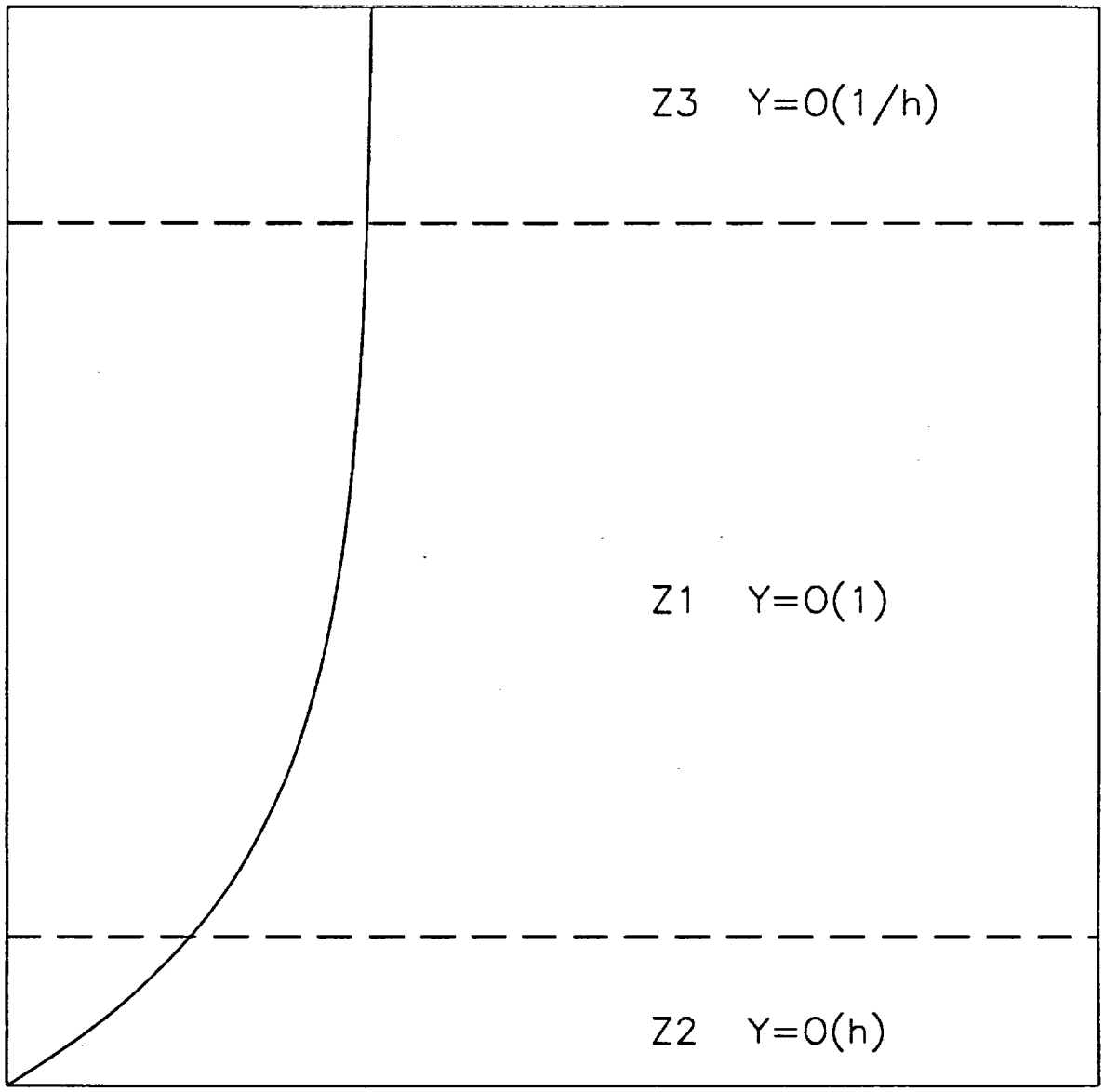

Figure 1 A sketch showing the regions Z1-Z3.

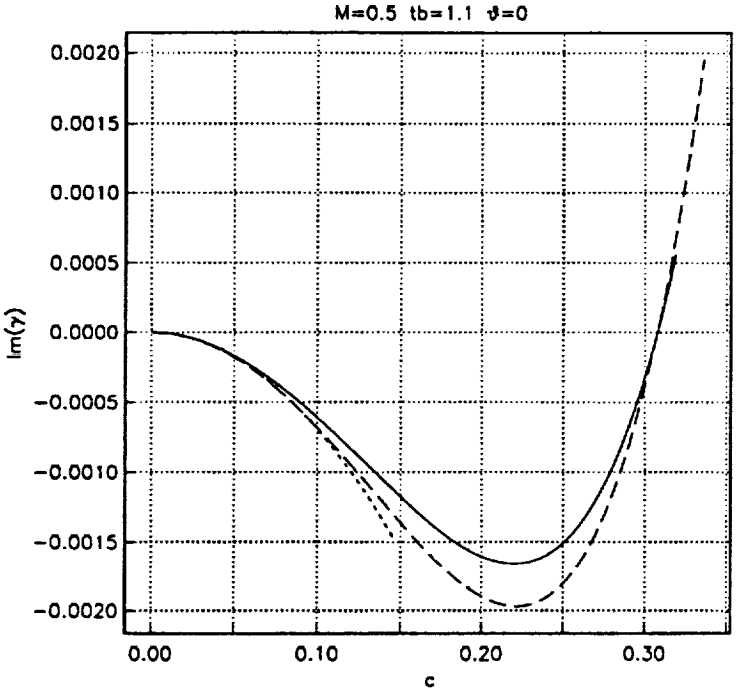

Figure 2a

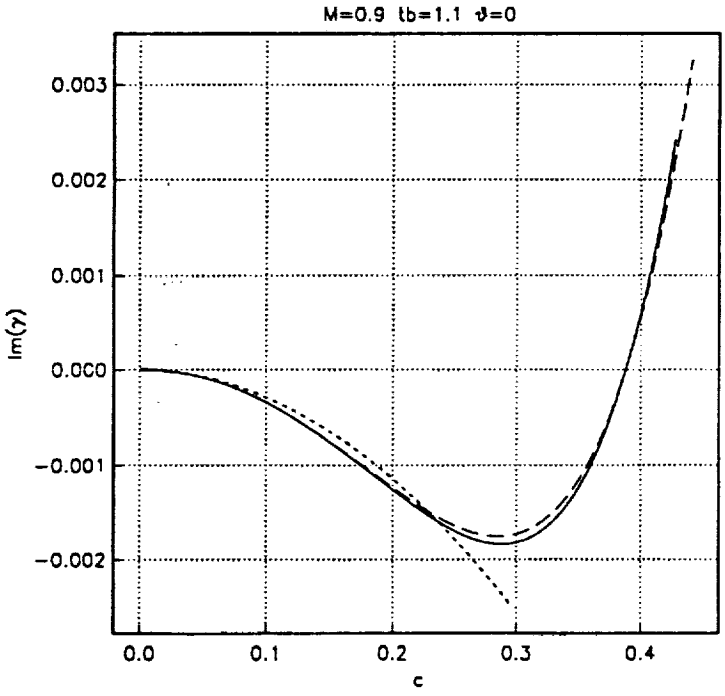

Figure 2b

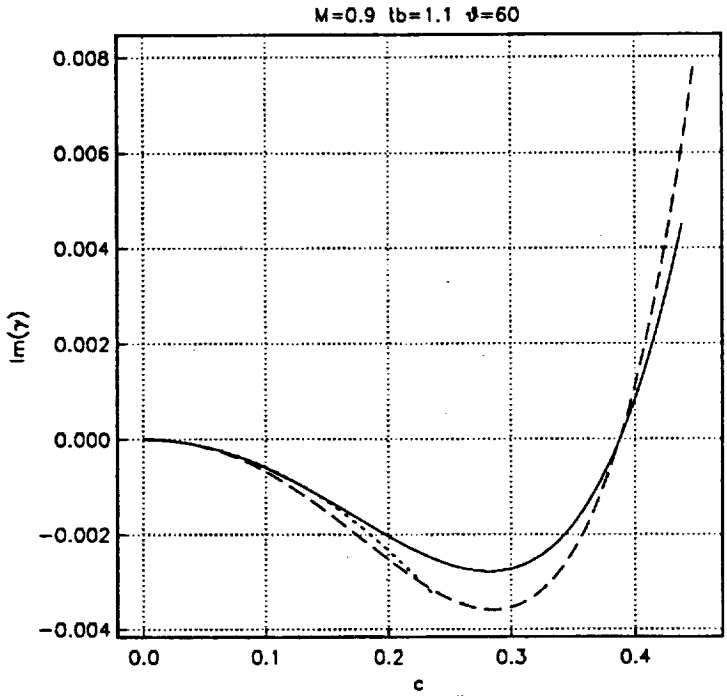

Figure 2c

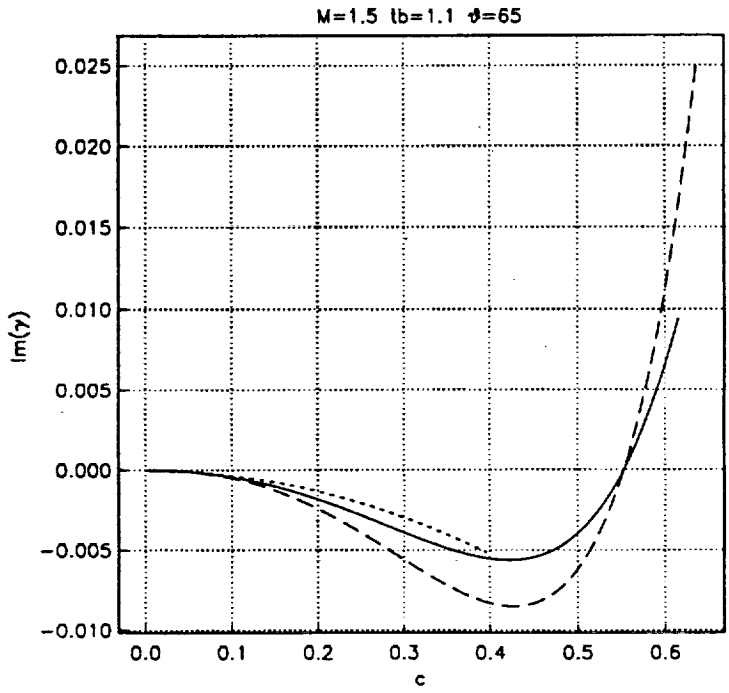

Figure 2d

Figures 2(a-d) Comparisons of the imaginary part of the waveneumber γ_* versus the phase speed c_* from the full numerical solutions of the linear Rayleigh problem (solid line), with asymptotic results, see the text. The thicker dashed line is the generalised expression (4.12a), the thinner dashed line the asymptote (4.11a) for the non-insulated case. The parameter $t_b = 1.1$. $M = M_\infty$ is the Mach number and θ the oblique angle.

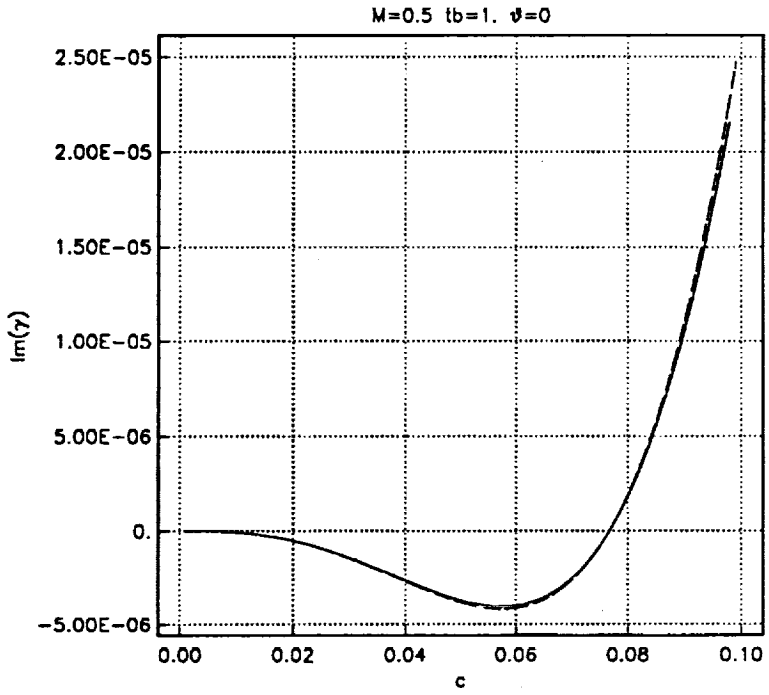

Figure 3a

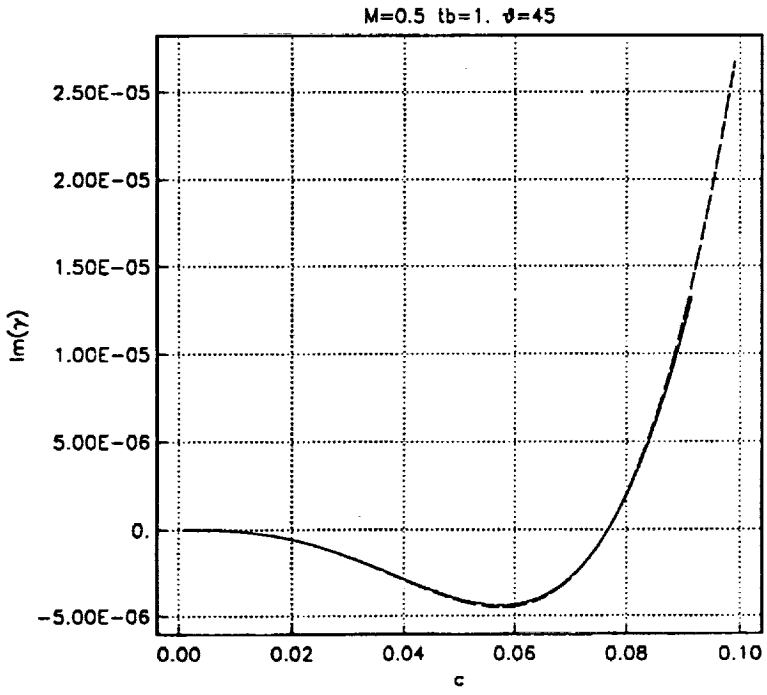

Figure 3b

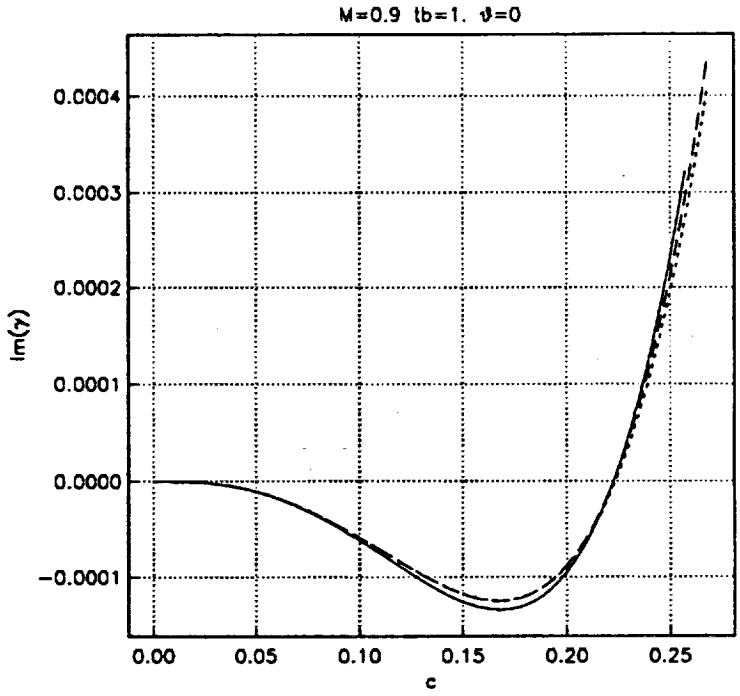

Figure 3c

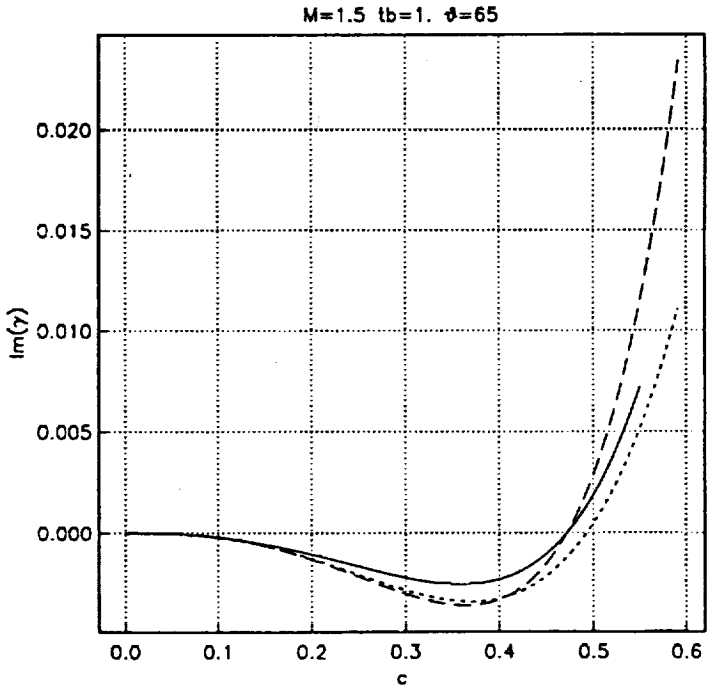

Figure 3d

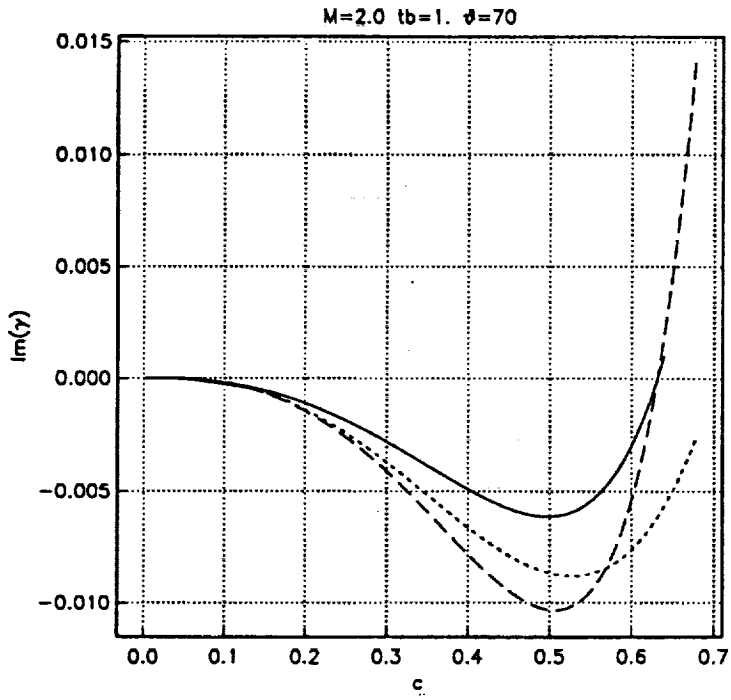

Figure 3e

Figures 3(a-e) As in Figure 2 except that the thinner dashed line is (4.12c) for the insulated case. Also $t_b = 1$.

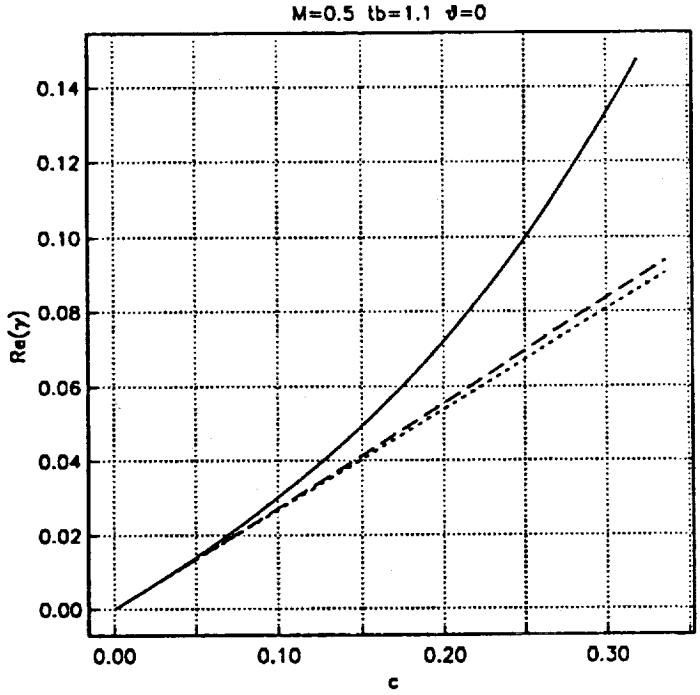

Figure 4a

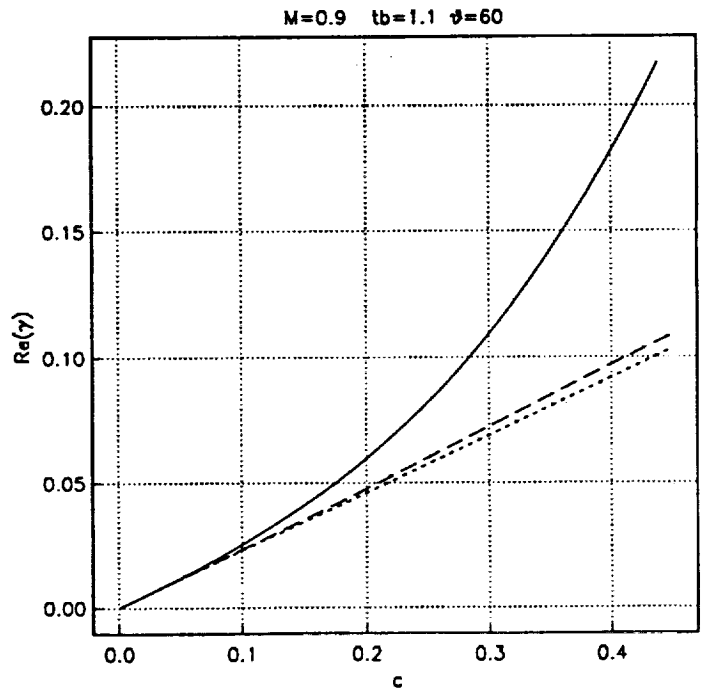

Figure 4b

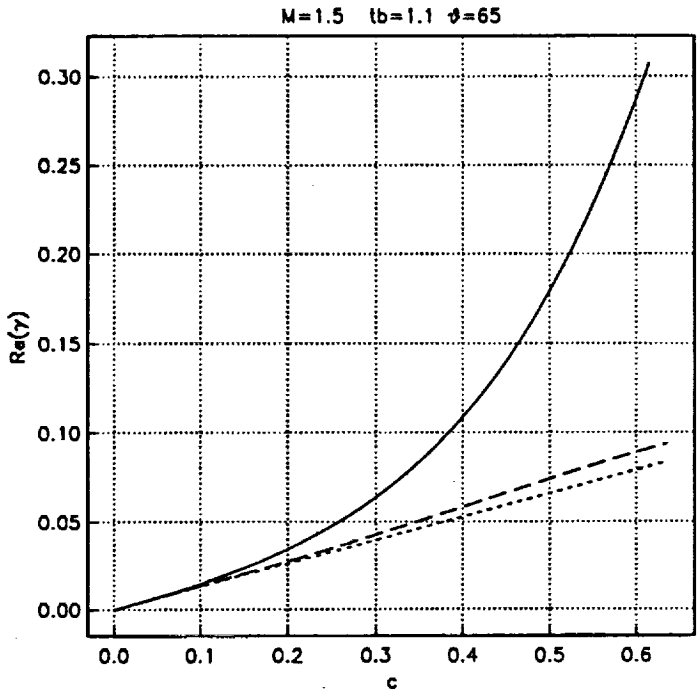

Figure 4c

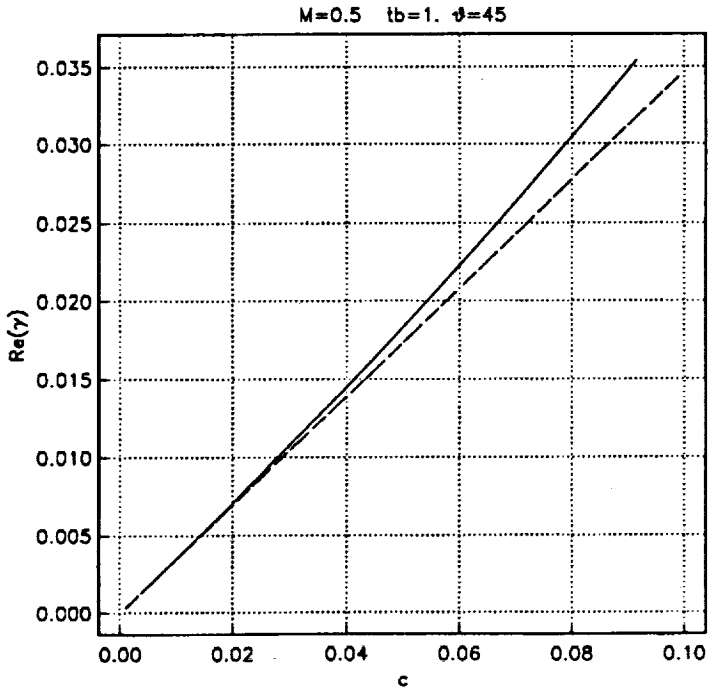

Figure 4d

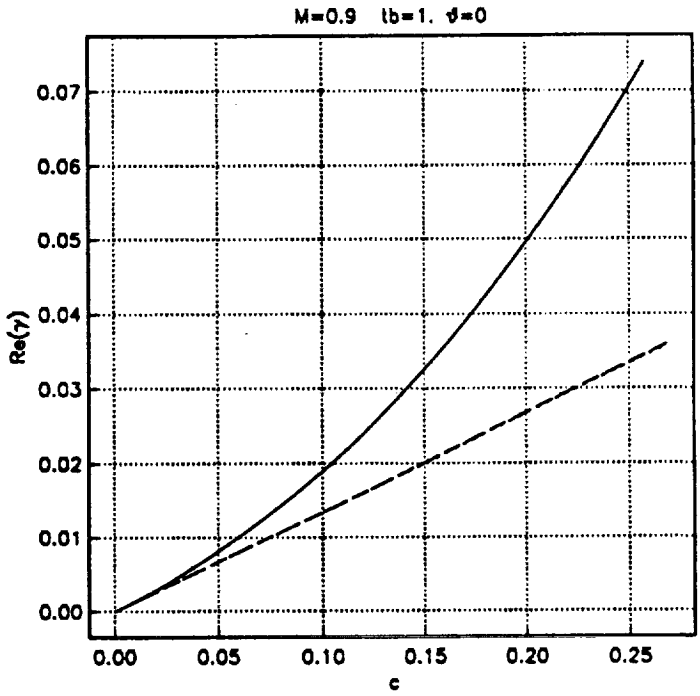

Figure 4e

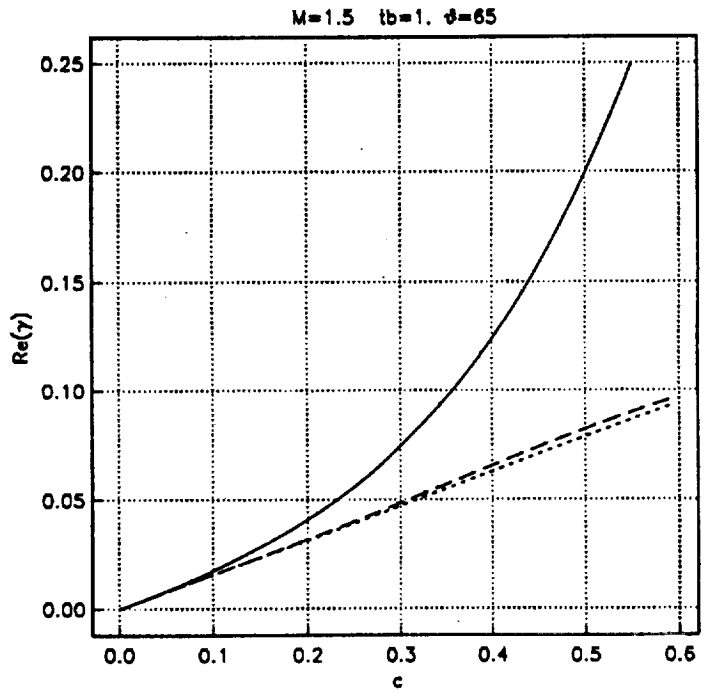

Figure 4f

Figures 4(a-f) Comparisons of the real part of the wavenumber from full numerical solutions of the Rayleigh problem (solid line) with the asymptotes (4.12b) (thicker dashed line) and (4.10) (thinner dash). Other parameter as in Figure 2.

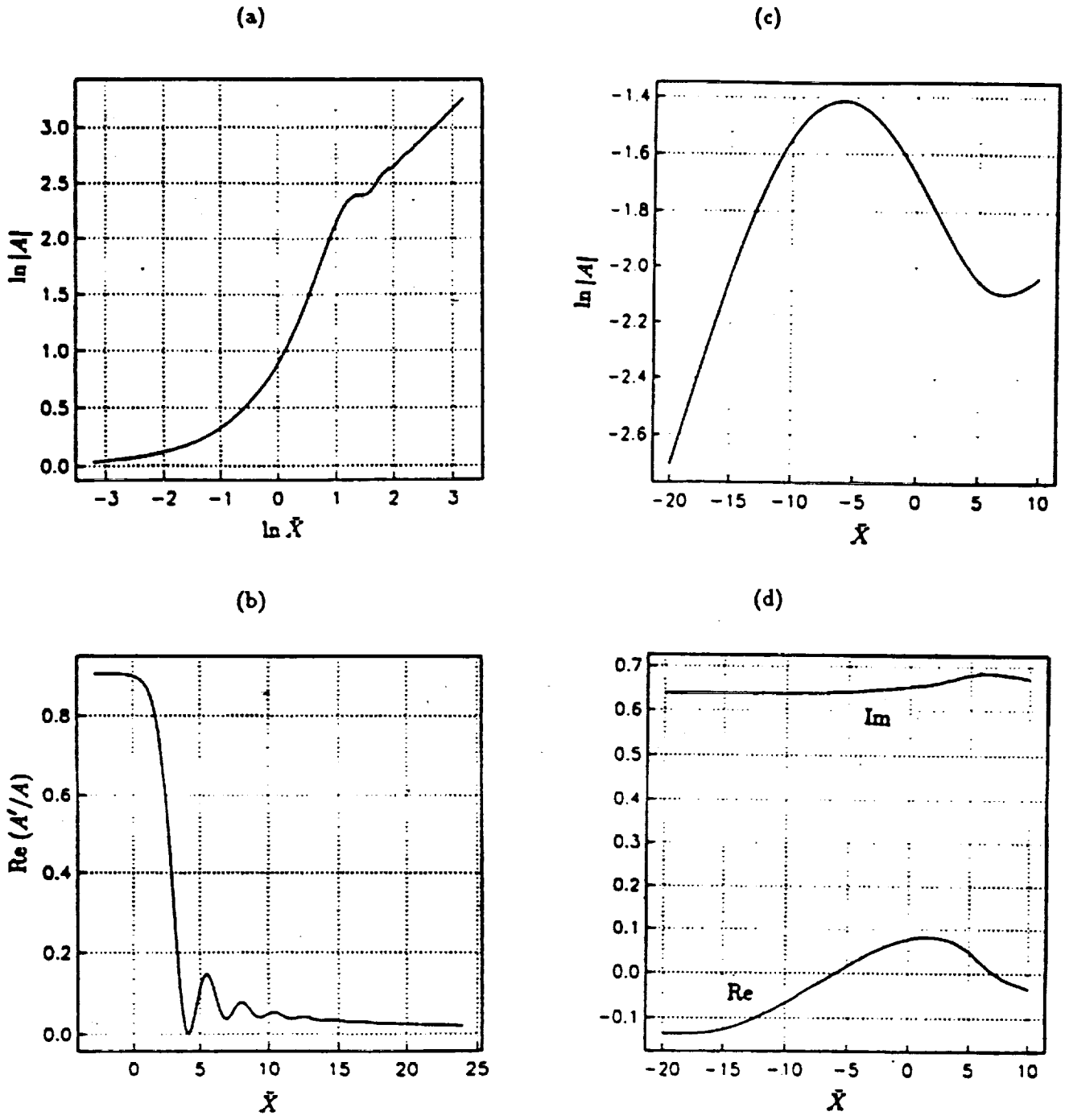

Figure 5(a-b) (a) A plot of the scaled wave amplitude A and (b) the scaled growth rate $Re(A'/A)$, as a function of the the spatial coordinate $\bar{X}$ for the Goldstein & Hultgren (1988) problem (see text) with $\gamma_c = 1$ and $U = 1$.

Figure 5(c-d) As in Figure 5(a) except $\gamma_c = 0$, and $U = 3$. In Fig. 5(d) the real and imaginary parts of $-A'/A$ are plotted.

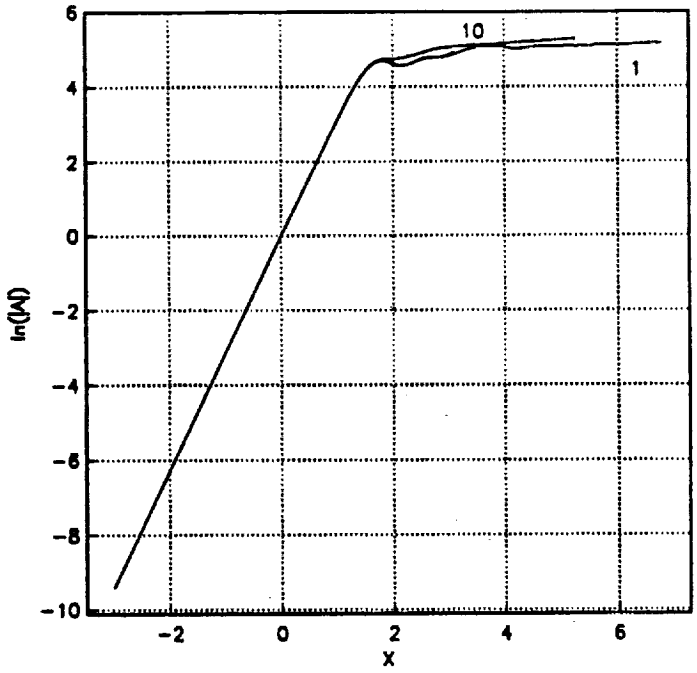

Figure 6a

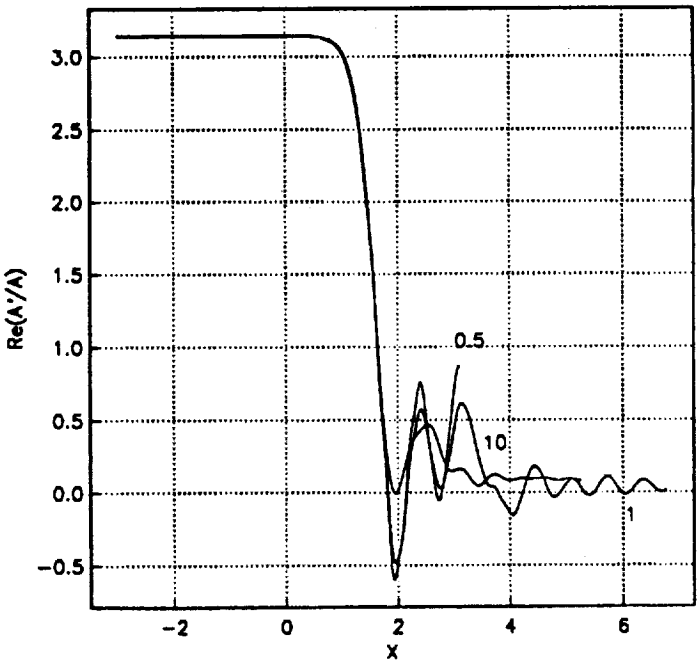

Figure 6b

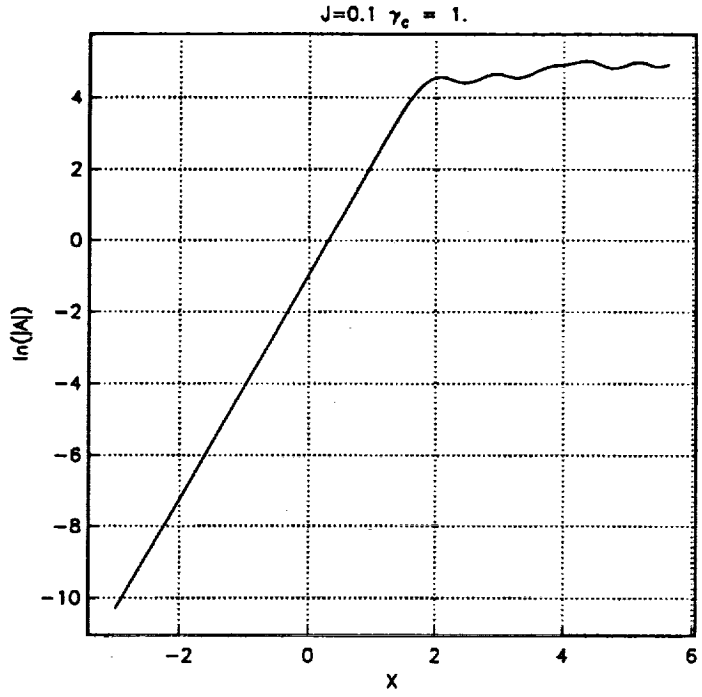

Figure 6c

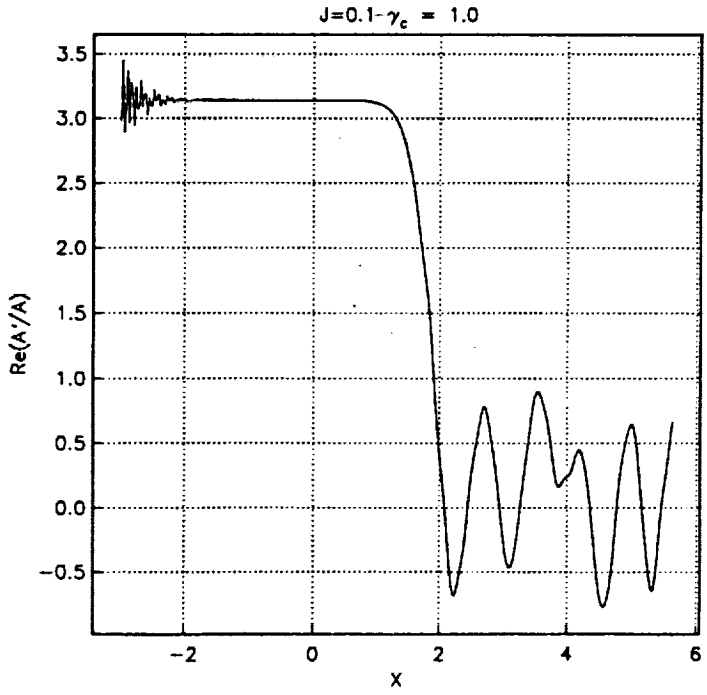

Figure 6d

Figure 6(a-b) Solution of the nonlinear problem (4.7) and the figures show the evolution of the scaled wave amplitude as a function of $\bar{X}$. The different curves are for $\gamma_c =$ 10, 1 and 0.5 with $J = 0$.

Figure 6(c-d) As in Figures 6(a-b) except $J = 0.1, \gamma_c = 1$.

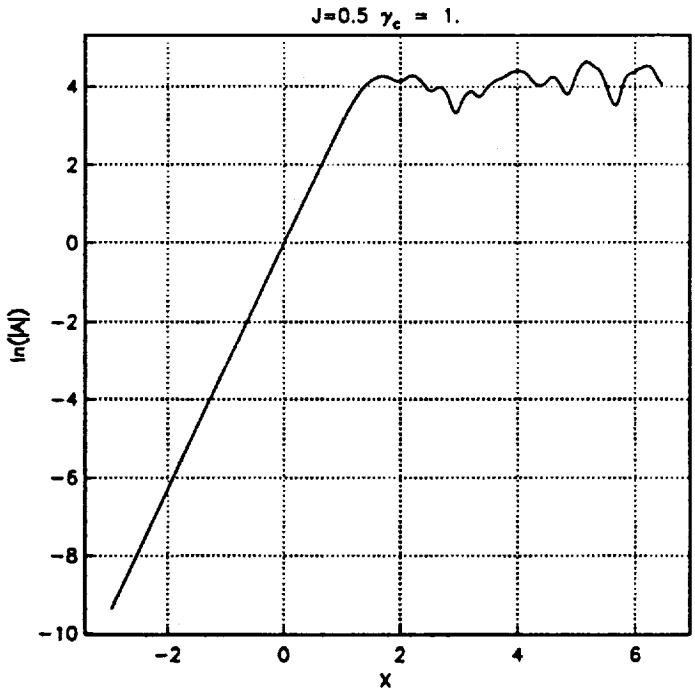

Figure 7a

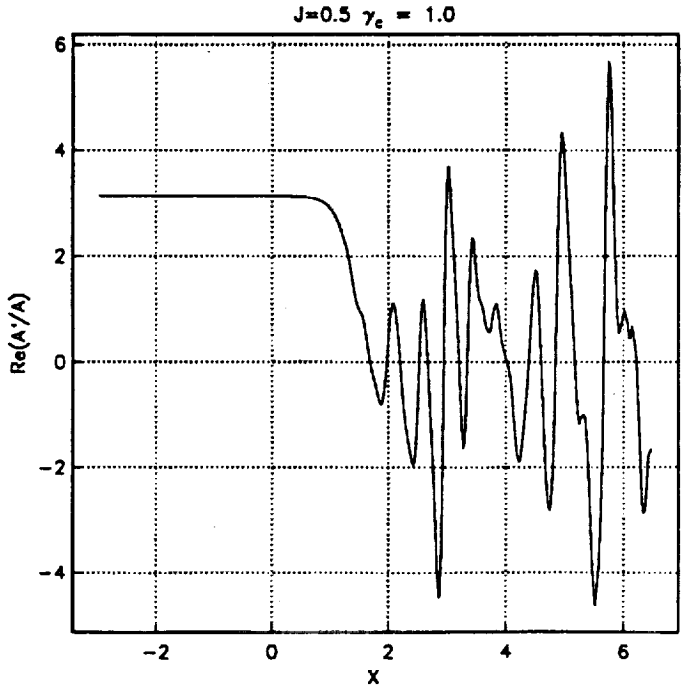

Figure 7b

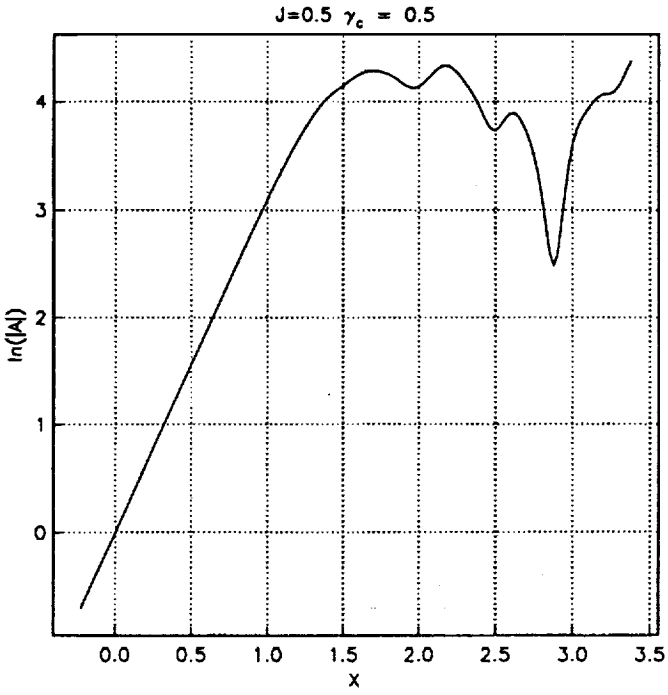

Figure 7c

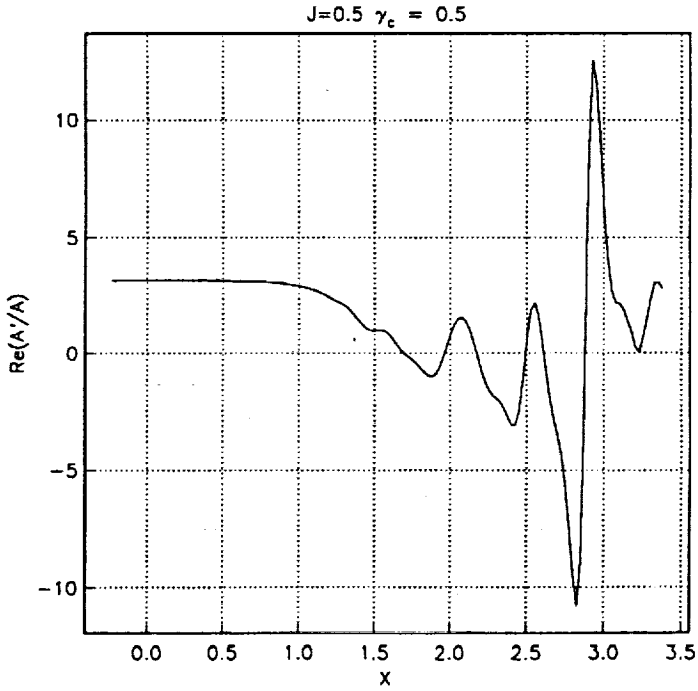

Figure 7d

Figures 7(a-d) As in Figures 6 except that (a-b) $J = 0.5, \gamma_c = 1$, (c-d) $J = 0.5, \gamma_c = 0.5$.

REPORT DOCUMENTATION PAGE

Form Approved
OMB No. 0704-0188

1. AGENCY USE ONLY (*Leave blank*)	2. REPORT DATE	3. REPORT TYPE AND DATES COVERED
	March 1993	Technical Memorandum

4. TITLE AND SUBTITLE

Nonlinear Evolution of the First Mode Supersonic Oblique Waves in Compressible Boundary Layers. Part I–Heated/Cooled Walls

5. FUNDING NUMBERS

WU–505–62–21

6. AUTHOR(S)

J.S.B. Gajjar

7. PERFORMING ORGANIZATION NAME(S) AND ADDRESS(ES)

National Aeronautics and Space Administration
Lewis Research Center
Cleveland, Ohio 44135–3191

8. PERFORMING ORGANIZATION REPORT NUMBER

E–7718

9. SPONSORING/MONITORING AGENCY NAMES(S) AND ADDRESS(ES)

National Aeronautics and Space Administration
Washington, D.C. 20546–0001

10. SPONSORING/MONITORING AGENCY REPORT NUMBER

NASA TM–106087
ICOMP–93–08

11. SUPPLEMENTARY NOTES

J.S.B. Gajjar, Mathematics Department, The University of Manchester, Manchester, M13 9PL, England, and Institute for Computational Mechanics in Propulsion, Lewis Research Center (work funded under NASA Cooperative Agreement NCC3–233). ICOMP Program Director, Louis A. Povinelli, (216) 433–5818.

12a. DISTRIBUTION/AVAILABILITY STATEMENT

Unclassified - Unlimited
Subject Category 34

12b. DISTRIBUTION CODE

13. ABSTRACT ***(Maximum 200 words)***

The nonlinear stability of an oblique mode propagating in a two-dimensional compressible boundary layer is considered under the long wave-length approximation. The growth rate of the wave is assumed to be small so that the ideas of unsteady nonlinear critical layers can be applied. It is shown that the spatial/temporal evolution of the mode is governed by a pair of coupled unsteady nonlinear equations for the disturbance vorticity and density. Expressions for the linear growth rate show clearly the effects of wall heating and cooling, and in particular how heating destabilizes the boundary layer for these long wavelength inviscid modes at O(1) Mach numbers. A generalized expression for the linear growth rate is obtained and is shown to compare very well for a range of frequencies and wave-angles at moderate Mach numbers with full numerical solutions of the linear stability problem. The numerical solution of the nonlinear unsteady critical layer problem using a novel method based on Fourier decomposition and Chebychev collocation is discussed and some results are presented.

14. SUBJECT TERMS	15. NUMBER OF PAGES
Critical layers; Compressible; Boundary-layer stability	32
	16. PRICE CODE: A03

17. SECURITY CLASSIFICATION OF REPORT	18. SECURITY CLASSIFICATION OF THIS PAGE	19. SECURITY CLASSIFICATION OF ABSTRACT	20. LIMITATION OF ABSTRACT
Unclassified	Unclassified	Unclassified	